ORIGINAL PAPER

Environmental life cycle assessment and operating cost analysis of a conceptual battery hybrid-electric transport aircraft

Anna Elena Scholz[1] · **Dimitar Trifonov**[1] · **Mirko Hornung**[1]

Abstract

Noise and greenhouse gas emission targets set by e.g., the EU commission, NASA, and ICAO oblige the aviation industry to reduce its environmental footprint. Battery-powered hybrid-electric aircraft are currently being investigated in this regard as they can potentially reduce in-flight greenhouse gas emissions and noise. However, most studies to date have focused on the CO_2 emission reduction potential instead of considering the total life cycle environmental impact. Hence, within this study an environmental life cycle assessment method for a hybrid-electric aircraft is developed and applied, supplemented by a direct operating costs analysis. This allows the simultaneous evaluation of the environmental impact reduction potential and the economic consequences for aircraft operators. This demonstrates the faced trade-off and contributes to a meaningful review process. A single-aisle transport aircraft (A320 class) serves as a use case for the established methodology. It consists of the conceptual aircraft design, the environmental life cycle assessment, and the direct operating costs analysis for a conventional reference aircraft and a hybrid-electric aircraft with a discrete parallel powertrain architecture. It should be noticed that the focus of this study is the comparison of conceptual aircraft designs of the same fidelity on system level, in lieu of the detailed modeling of a hybrid-electric aircraft. Results show that for a degree of hybridization of 0.3, the environmental impact of the hybrid-electric configuration increased by 15.1%, while the operating costs increased by 41.0% compared to a conventional reference aircraft. For a future scenario, favourable for hybrid-electric aircraft with i.a. renewable electricity production, the environmental impact could be reduced by 7.0% compared to the reference aircraft. At the same time, the operating costs gap between both configurations decreases to +26.8%. Hybrid-electric aircraft should therefore be investigated further as a potential solution to reduce the environmental impact of aviation, if simultaneously to developing them the expansion of renewable energies is fostered. Nevertheless, this reduction in environmental impact involves a high direct operating costs penalty.

Keywords Hybrid-electric aircraft · Aircraft design · Environmental life cycle analysis · Operating costs

Nomenclature

Symbols

BPR	Bypass ratio, -
C	Cost, €
f	Portion/factor, -
H	Degree of hybridization, -
k	Country specific parameter, -
l	Length, m
L	ICAO certified noise level, EPNdB
m	Mass, kg
OPR	Overall pressure ratio, -
r	Radius, m
R	Range, km
R^2	Coefficient of determination
T	Thrust, kN
T	Noise threshold value, EPNdB
U	Unit cost rate, €/noise unit or €/kg

Subscripts

a	Arrival
adj	Adjusted
cl,toll	Climate toll
d	Departure

✉ Anna Elena Scholz
anna.scholz@tum.de

Dimitar Trifonov
dimitar.trifonov@yahoo.com

Mirko Hornung
mirko.hornung@tum.de

[1] Institute of Aircraft Design, Technical University of Munich, Boltzmannstr. 15, 85748 Garching, Germany

DF	Ducted fan
E	Energy
ETS	Emissions trading system
flight	During the flight
LTO	Landing and take-off
mission	Of the mission
noise	Noise
TF	Turbofan
total	Total
0	Maximum rated

Abbreviations

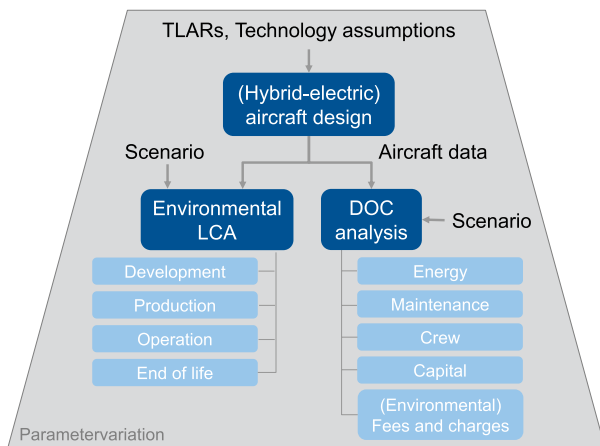| AC | Alternating current |
ADAC	Allgemeiner Deutscher Automobil-Club e.V. (German automobile club)
ADEBO	Aircraft Design Box
AEA	Association of European Airlines
ATA	Air Transport Association of America
AVL	Athena Vortex Lattice
CeRAS	Central reference aircraft data system
CG	Center of gravity
CRA	Conventional reference aircraft
DC	Direct current
DLR	Deutsches Zentrum für Luft- und Raumfahrt
DOC	Direct operating costs
EASA	European Union Aviation Safety Agency
EIS	Entry into service
ELCD	European reference life cycle database
EM	Electric motor
ERLIG	Emissions Related Landing Charges Investigation Group
ETS	Emissions trading system
GDP	Gross domestic product
HEA	Hybrid-electric aircraft
IATA	International Air Transport Association
ICAO	International Civil Aviation Organization
LCA	Life cycle assessment
LTO	Landing and take-off
L/D	Lift-to-drag ratio
MTOM	Maximum take-off mass
NASA	National Aeronautics & Space Administration
OECD	Organisation for Economic Cooperation & Development
OEM	Operating empty mass
PKM	Passenger-kilometer
PMAD	Power management and distribution
PVC	Polyvinyl chloride
SS	Single score (result of the LCA)
SUGAR	Subsonic ultra green aircraft research
TLAR	Top level aircraft requirement
TSFC	Thrust-specific fuel consumption
XLPE	Cross-linked polyethylene

1 Introduction

Growing air traffic passenger volumes [1], but at the same time increasing environmental awareness and targets for greenhouse gas emission and noise reductions set by several advisory bodies, highlight the need of the aviation industry to constantly improve and reduce its environmental impact. Research institutes and industry are therefore currently examining and exploiting different technology and aircraft configuration options. Among others, hybrid-electric aircraft (HEA) are seen as a promising candidate to achieve the specified emission and noise goals.

Previous studies have undertaken conceptual designs of possible future hybrid-electric transport aircraft, exploiting the different alternatives hybrid-electric configurations offer (e.g., serial hybrid, parallel hybrid, discrete parallel hybrid, etc.). However, so far only the CO_2 emissions and direct operating costs (DOC) of the respective design missions were evaluated (see e.g., [2–6]). Nevertheless, to establish a meaningful review of HEA, a complete life cycle analysis (LCA) regarding the environmental impact is necessary. Furthermore, in order to be able to truly assess the DOC, environmental airport charges (emissions and noise) should be included. They are likely to increase for conventional jet engine aircraft in the future, and thus might be decisive for airlines. Hence, the aim of this paper is to undertake an environmental LCA and a DOC analysis for a hybrid-electric, single-aisle aircraft including the aforementioned shortcomings of previous studies. The objective of the study is then to determine if, and under which circumstances, hybrid-electric transport aircraft are a valuable solution, from both an environmental and an economic point of view, to reduce the climate impact of the aviation industry. Thus, the scope is the system level assessment of conceptual aircraft designs of the same fidelity level showcasing potential benefits/drawbacks of HEA, rather than the detailed modeling of an HEA.

2 Methodology

The proposed methodology is outlined in Fig. 1. First, a conventional reference aircraft (CRA) and an HEA are designed using the in-house aircraft design environment ADEBO [7]. In a next step, an environmental LCA model is established to assess CRA and HEA and then applied to the designed aircraft. Similarly, a DOC methodology including environmental charges is developed and applied. Trade-offs are then identified using parameter variations for the design variables (e.g., degree of hybridization) and technology assumptions (e.g., battery specific energy). A future scenario is also investigated.

Fig. 1 Established methodology

Fig. 2 Discrete parallel hybrid architecture (cross-link via generator is optional)

The established information is used to determine the conditions under which hybrid-electric transport aircraft might be a sensible solution to reduce the environmental footprint of aviation, and at the same time be economically compelling for aircraft operators.

In the following sections, the three main parts of the established methodology are explained in more detail: the aircraft design in ADEBO, the environmental life cycle analysis model, and the direct operating costs model.

2.1 Aircraft design with ADEBO

The aircraft design environment ADEBO has been developed at TU Munich and allows conceptual design studies for all fixed-wing configurations. Besides transport aircraft, this also includes unmanned aerial vehicles and fighter aircraft. Both its object-oriented data model and its modular, tool-based implementation in MATLAB permit a high flexibility and extensibility for new concepts. Alongside tools based on semi-empirical handbook methods, interfaces exist to physics-based tools. These include in-house tools implemented in MATLAB, as well as external tools such as the aerodynamic analysis program Athena Vortex Lattice (AVL) by Drela [8], which are run in batch mode. More detailed information about ADEBO, its data model and capabilities can be found in [7].

Both the design of the CRA and of the HEA are undertaken using ADEBO. Within this study single-aisle transport aircraft are considered. The conventional design process follows a sizing methodology similar to the one explained in [7]. In order to establish a sizing methodology for the HEA, its propulsion architecture first has to be chosen. Mainly three different possibilities exist as discussed in e.g., [2, 9–12]: a series hybrid, a parallel hybrid and a discrete parallel hybrid architecture.
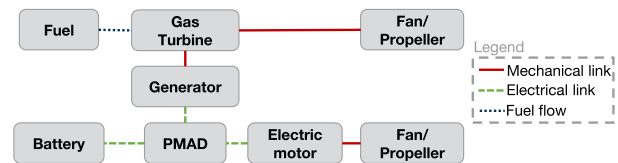
In the series architecture, the coupling between the conventional and the electric powertrain is achieved electrically via a power management and distribution (PMAD) system. Its advantage lies in the decoupling of thrust generation and power generation. In this manner enabling a flexible location of the gas turbine and a distributed electric propulsion. Nevertheless, the series hybrid architecture is comparably heavy: a gas turbine, a generator, and an electric motor are required, each sized for the maximum power demand.

Coupling the powertrains mechanically leads to the parallel hybrid architecture. No generator is required here, making it lighter than the series architecture. However, the mechanical coupling (probably a gearbox) is complex, adding to the weight. Another major drawback arises from running the electric motor and the gas turbine on one single shaft. This possibly leads to a more dynamic use of the gas turbine and hence part-load operation that decreases efficiency.

The third possible architecture is the discrete parallel hybrid. It is a combination of the two previously described architectures (see Fig. 2). In principle, both powertrains are decoupled from each other and provide a share of the required thrust. Optionally, they can be coupled via a generator to extend the systems capabilities. For example, to provide a means to run the system like a series architecture or charge the batteries during flight.

Within the scope of this paper, it was decided to implement a discrete parallel hybrid architecture with two turbofans and two electric ducted fans, but without the optional generator (thus no direct coupling). This architecture has the advantage that it is relatively easy to implement in the existing software framework. It is thus ideal to test the capabilities of handling HEA in ADEBO. Nevertheless, it should be noted here that besides the mentioned advantage for this study, this architecture does not exploit as many possible synergistic effects for HEA, as would be possible with other architectures. With the series hybrid architecture, for example, distributed electric propulsion could be realised.

Considerable changes have been introduced in the design process of the CRA to account for the hybrid-electric propulsion system and its architecture. The resulting HEA sizing methodology is shown in Fig. 3.

To begin with, the top level aircraft requirements (TLARs) (e.g. payload, range, etc.), initial assumptions and the design
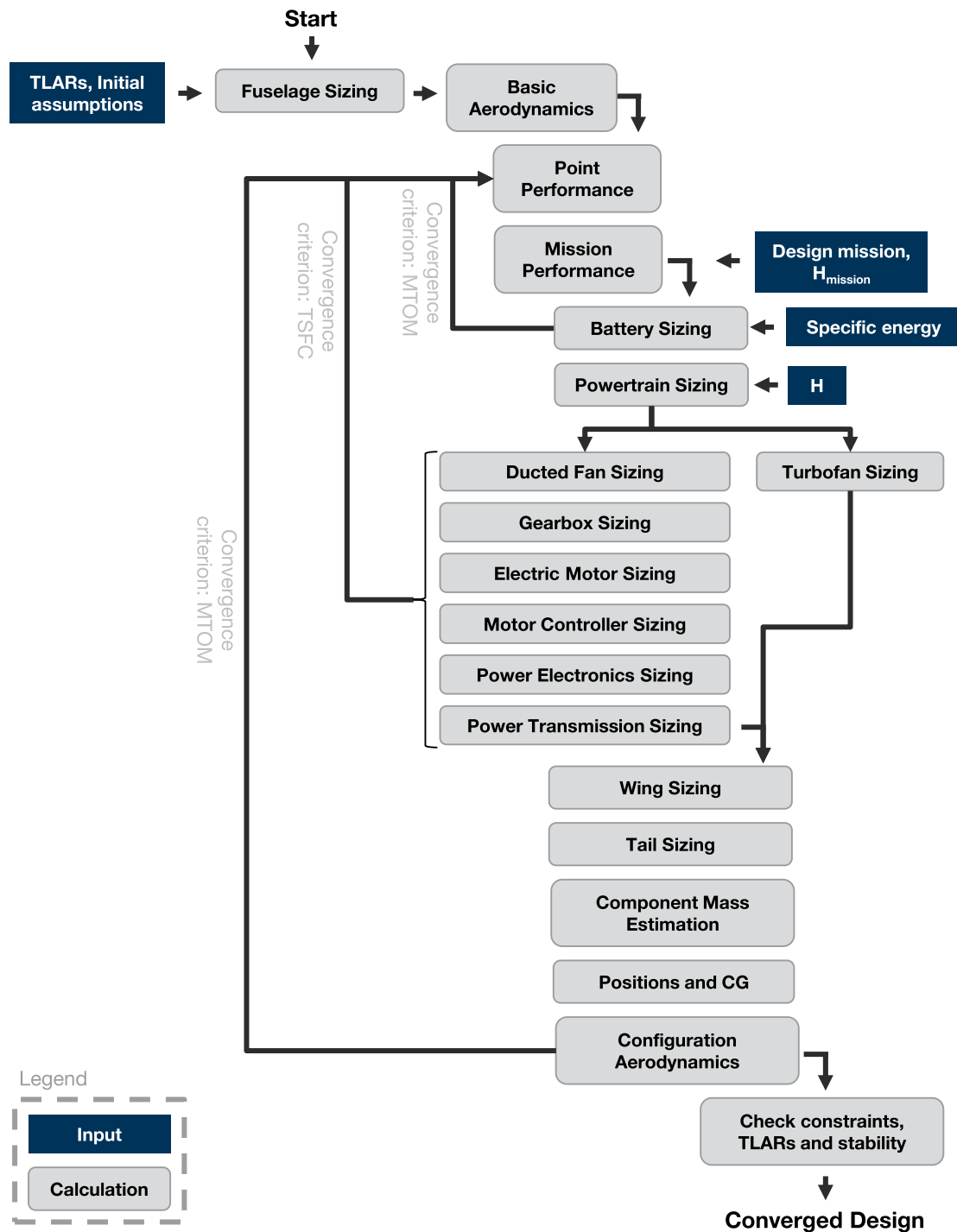
Fig. 3 HEA sizing methodology implemented in ADEBO

variable values are specified by the user. The program execution starts with the fuselage design and handbook-based, basic aerodynamic estimations. In the point performance module, constraints are evaluated and a required thrust-to-weight ratio and wing loading are determined. Together with the initial estimate of the maximum take-off mass (MTOM), the wing

area and the sea level thrust can then be calculated. In the mission performance and battery sizing modules, a "hybridized" version of the fuel fraction method by [13] (generally speaking, a power fraction method) is used. It calculates initial battery mass, fuel mass, operating empty mass (OEM) and a new MTOM based on the specified design mission and

thrust degree of hybridization H_{mission} per mission segment (operating strategy). The first iteration loop aims to achieve a convergence of these tools in terms of MTOM.

Once it has converged, the powertrain sizing is undertaken. Depending on the chosen overall thrust degree of hybridization H, the total required thrust is divided into a thrust requirement for the electric ducted fan T_{DF} and for the turbofan T_{TF}.

$$H = \frac{T_{\text{DF}}}{T_{\text{DF}} + T_{\text{TF}}} = \frac{T_{\text{DF}}}{T_{\text{total}}} \tag{1}$$

In the following, the turbofan is designed and thrust tables are calculated for off-design conditions. Similarly, the electric ducted fan is designed and the off-design points are evaluated. Consequently, the gearbox and the electric motor are sized for the maximum power expected during operating conditions. Likewise, the motor controller, power electronics and power transmission are sized. The respective sizing models for these components will be described in detail in the following sections. The second iteration loop has the thrust-specific fuel consumption (TSFC) as convergence criterion.

The wing and tail are then sized and the component masses are estimated (handbook-methods, e.g., from [14, 15] are used for structural components, systems and operating equipment, while the powertrain component masses are estimated with methods described in the following sections). The OEM (and the MTOM respectively) are then updated. Next, the positions of the individual components are assigned and the wing (and associated components) positions are iterated to obtain a user-specified center of gravity (CG) position of the empty aircraft [14]. In a last step, the configuration aerodynamics are determined using (1) the vortex lattice program AVL (as described above [8]), (2) the drag component build-up method by Raymer to account for zero-lift drag [16], and (3) the transsonic wave drag estimation by Malone and Mason [17]. In this way, differences in wetted area of the CRA and the HEA due to different wing sizes and the electric ducted fans of the HEA, as well as integration effects of the electric ducted fans (interference with the wing) are captured in the design process.

The process is repeated with this information (with a more detailed mission performance module, including the calculated thrust and power tables and the configuration aerodynamics) until the MTOM converges. Finally, the top level, point performance, and stability requirements are once again checked.

2.1.1 Turbofan sizing

Previously, the sizing of the turbofans in ADEBO was undertaken by means of a so-called "rubber engine sizing", with sizing equations provided in [18]. However, these equations are only valid for $0 \leq \text{BPR} \leq 6$ and furthermore, are based

on 1976 data. Since the CRA of 2035 is expected to have a higher BPR, new sizing functions were derived.

A database of turbofan engines was compiled for this purpose that is based on the ICAO Aircraft Engine Emissions Databank of the 20th of September 2019. All engines which are out of service, are no longer produced or were tested before the start of 2000 were deleted. For the remaining engines, the EASA type-certificate data sheets were consulted. The dry mass, length and (average) diameter were collected. For seven of the engines, no type-certificate could be found online, hence they were subsequently deleted from the database. Consequently, a total of 220 turbofans is included in the database.

A statistical regression analysis was performed for the collected data with different independent variables to identify those with a high correlation. The resulting equations for the radius r_{TF}, length l_{TF}, and the mass m_{TF} all have a p-value lower than 0.2:

$$r_{\text{TF}}[\text{m}] = 0.5150 + 0.0241\,\text{BPR} + 3.2289 \cdot 10^{-3}\,T_0[\text{kN}] \tag{2}$$

$$R^2_{\text{adj}} = 0.9218$$

$$l_{\text{TF}}[\text{m}] = 2.2210 + 9.2589 \cdot 10^{-3} T_0[\text{kN}] \tag{3}$$

$$R^2_{\text{adj}} = 0.7454$$

$$m_{\text{TF}}[\text{kg}] = 118.5070 + 52.2266\,\text{BPR} + 17.4877\,T_0[\text{kN}] \tag{4}$$

$$R^2_{\text{adj}} = 0.9693$$

The adjusted R^2 values are quite large for radius and mass, but not so large for the length. However, no greater value could be achieved with the available independent variables (T_0, BPR, OPR). Since it is generally the diameter and not the length of the engine that plays a crucial role for the placement of the engine in the conceptual design, the R^2_{adj} value was deemed acceptable for this use case. Especially since the general trend is still depicted, as shown in Fig. 4.

Having derived equations for the dimensions and mass, a method for the performance analysis is still required. As the required information is not contained in the database or in the EASA type-certificate data sheets, the method for thrust and TSFC calculation for turbofans proposed by ([19], Sect. 3.6) is implemented. To account for changes in TSFC with changing BPR more precisely, the two values for the reference TSFC suggested for low and high BPR engines in [19] are refined. This is done by adjusting the output to the method described in [20] for different BPR.
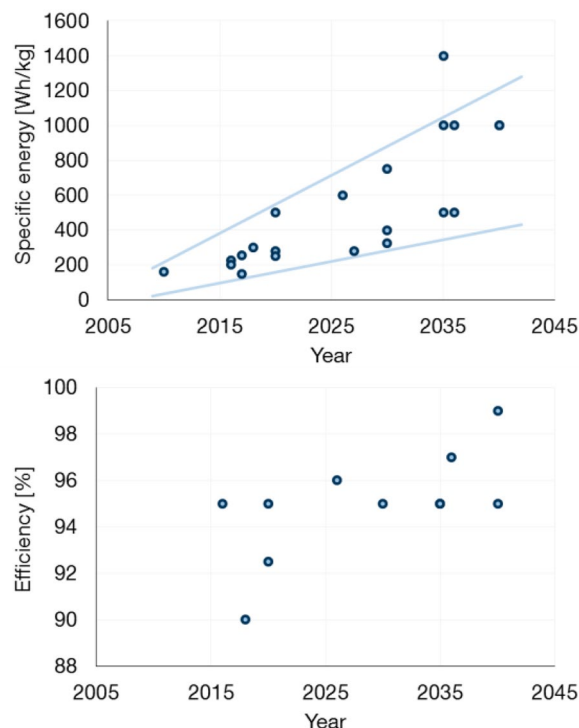
2.1.2 Battery sizing

As noted by many studies that consider batteries as energy providers in aircraft, the battery specific energy (energy content per unit mass) plays a decisive factor in the
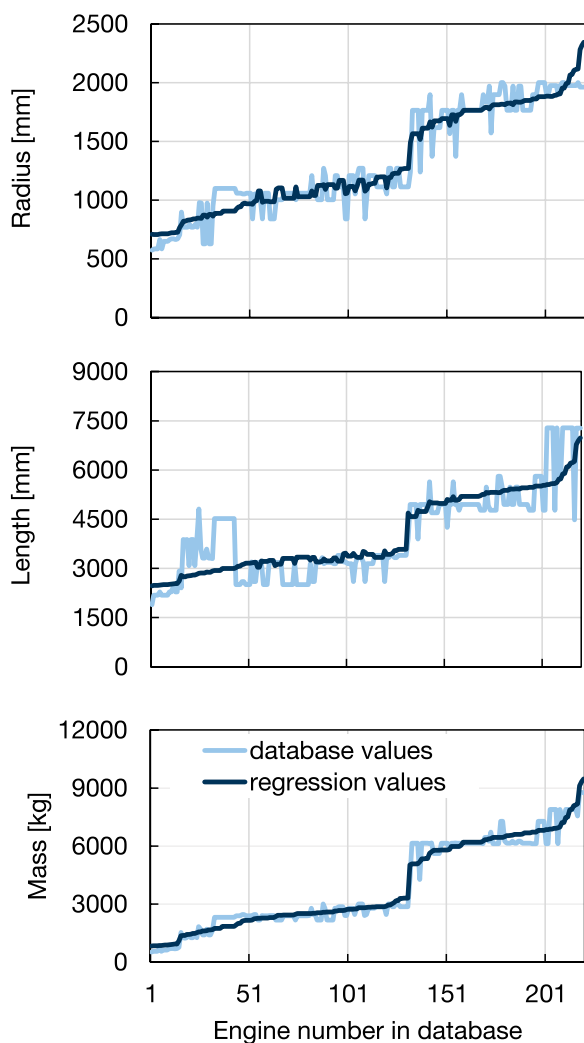
Fig. 4 Visual comparison of radius, length and mass of all engines in the database with the results of the regression functions

Fig. 5 Assumed and predicted battery specific energy and efficiency in various studies (data from: [2, 3, 9, 21, 23–30]). Note that it was not always stated if the specific energy was at cell or pack level. Where stated, the value at pack level was taken

aircraft sizing and depends on the battery technology level. State-of-the-art (in 2017) battery specific energy is around 0.27 kWh/kg (cell level) according to [21]. Comparing to the traditionally used kerosene as energy provider with a specific energy of about 12 kWh/kg [22], this leads to a factor of about 45 of difference (this comparison is based on the battery specific energy at cell level, making it likely that the factor will further increase when compared at system level). Even if the powertrain efficiencies are considered (e.g., 40% for the conventional powertrain and 65% for the electric powertrain), a factor of about 27 remains. Consequently, this makes battery-powered aircraft (even with a specific energy that is about four to six-times higher than state-of-the-art as assumed in this study) comparably heavy.

As pointed out in [3], the batteries' specific power is equally important. It might limit the power draw and could

therefore determine the operation strategy of the HEA. Nevertheless, the main focus of the battery sizing in this study is the specific energy, assuming that the battery allows the respective power draw.

Designing an aircraft for entry into service (EIS) in the next decades requires a prediction of the development of the battery technology. As accurate technology forecasts are difficult, a survey has been undertaken within this study. Battery specific energy and efficiency assumptions and predictions within aircraft design related studies have been collected. The results are visualized in Fig. 5. The assumptions for the specific energy show a clear upward trend when comparing the different studies. Even though this trend can also be seen for the efficiency, it is not as prominent.

A battery specific energy at pack level of at least 800 Wh/kg is required for a single-aisle, parallel HEA to achieve higher reductions in CO_2 emissions than its conventional, kerosene-powered counterpart ([9], p. 56). With this in mind, 1000 Wh/kg, 1250 Wh/kg and 1500 Wh/kg at pack level and a battery efficiency of 99% are chosen for the HEA parameter investigations in this study. Compared to the assumptions and predictions of other single-aisle HEA studies (e.g., 1400 Wh/kg for a 900 nmi mission ([29], p. 347) and

1000 Wh/kg for a 1000 nmi mission ([2], Tab. 1))[1], the baseline value for the specific energy of 1000 Wh/kg seems appropriate, yet still aggressive and optimistic. At the same time, the values for the parameter variations anticipate an even greater improvement in battery technology. Since the scope of this study is the comparison of two different aircraft concepts on system level assessing potential benefits and drawbacks of HEA, and not a detailed realistic design of an HEA, this is deemed suitable. For a long lifetime of the battery, its state of charge should not fall below 20%. This study assumed that this 20% additional electric energy could be used for the required mission reserves.

2.1.3 Power transmission sizing

Another vital component for the electric powertrain is the power transmission. For the scope of this study a conventional, non-superconducting power transmission is chosen as the technology readiness level of superconductivity is still very low ([31], Fig. 14). In order to minimize the electromagnetic interference and weight [31, 32], a direct current (DC) (instead of an alternating current (AC)) power distribution system is selected. The higher the system voltage level, the lower the associated power loss; however, concerns arise regarding safety and failures [31].

Vratny et al. studied the optimum system voltage for two different electric power architectures and concluded that it is in the range of 1–4 kV [33]. However, they did not evaluate whether these voltage levels are applicable to aircraft. Isikveren et al. in turn investigated voltage levels of 1–3 kV for the all-electric aircraft concept Ce-Liner [32] and adopted a voltage level of 3 kV [29]. Stückl et al. designed the all-electric aircraft concept Voltair assuming a voltage level of 1 kV [34]. Pornet et al. selected a system voltage level of 3 kV for their HEA study [29], while Wroblewski et al. opted for 1 kV for their HEA design study [4]. A voltage level of 1 kV has been chosen in this study.

The cable sizing in terms of mass and efficiency is realized using the methodology explained in ([35], Sect. 3.1.2.1). The only difference is the altered gravimetric density of the isolation material XLPE of 0.923 g/cm^3 [36], as the one used in Stückl (1.4 g/cm^3) seemed to be very high compared to other sources. Stückl calculates the cable mass per length in terms of the required conductor cross-section, the isolation and sheath thicknesses, and the respective gravimetric densities of their materials. In this study, an additional installation weight factor of 1.15 is assumed, accounting for the extra material to mount the cables in the aircraft. The efficiency, or power loss per length of the cable, is calculated using the

resistivity characteristic of the chosen conductor material and the operating temperature.

Today's most prevalent conductor materials are aluminium and copper. They differ in terms of their conductivity (copper has a higher conductivity) and their gravimetric density (aluminium has a lower density). Thus, depending on the use case, one or the other is chosen. The trade study for a parallel HEA at aircraft level in [2] concluded that aluminium is preferable in terms of block fuel consumption. Hence, for the HEA of this study, aluminium was chosen as a conductor material. As suggested by Stückl, XLPE is chosen for the isolation material and PVC for the sheath [35].

2.1.4 Power electronics sizing

To ensure safe and reliable power conversion and distribution, power electronics such as circuit breakers, converters, rectifiers, inverters and motor controllers are required. They are part of the PMAD system on-board the aircraft.

One important consideration to be made when choosing the individual components is the occurrence of electric arcing, due to isolation faults of ageing cables [37], for example. According to Paschen's law, at sea level pressure electric arcing can develop in air above voltages of 327 V. Reducing the pressure (i.e., by flying at a higher altitude than sea level) means that electric arcing becomes more critical [35]. Varying temperature and moisture content during a flight cycle and the lifetime of an aircraft add to the problem [38]. Particularly important is that no voltage zero-crossing interrupts the arcing in a DC system. Consequently, a continuous arc that is prone to cause even more damage and fire hazard develops. Hence, this phenomenon has to be accounted for when selecting the individual power electronic components for the chosen system (DC, voltage level of 1 kV; see Sect. 2.1.3).

However, as the goal of this study is a conceptual design of an HEA, it was decided that a rough estimate of the performance and mass of the power electronics is sufficient here. Hence, the same specific power and efficiency for all power electronics is chosen. A respective literature survey considering aircraft design related studies is undertaken (see Fig. 6).

Analyzing the results of the survey as depicted in the figure, it can be seen that despite comparing values for all kinds of power electronics, the values still have a similar magnitude. The approach of "taking one value for all" can thus be regarded as acceptable. A specific power of 15 kW/kg and an efficiency of 97% is chosen, in-line with the literature.

2.1.5 Electric motor sizing

The electric motor is used to convert the electrical power provided by the battery into rotational mechanical power,

---

[1] As outlined in Chap. 3, a single-aisle aircraft of A320/B737 class is considered as a use case in this study.
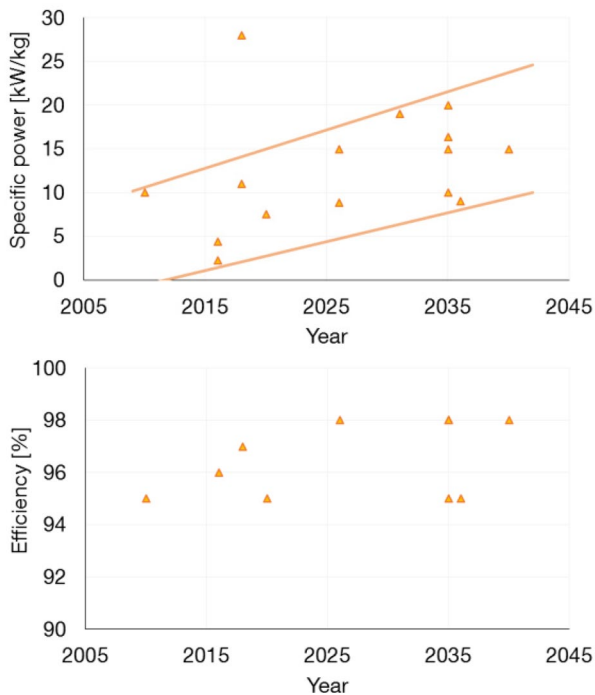
Fig. 6 Assumed specific power and efficiency of power electronics in various studies (data from: [3, 9–11, 24, 26, 27, 39])

Fig. 7 Assumed specific power and efficiency of electric motors (non-superconducting) in various studies (data from: [3, 9–11, 23–27, 31, 39, 42])
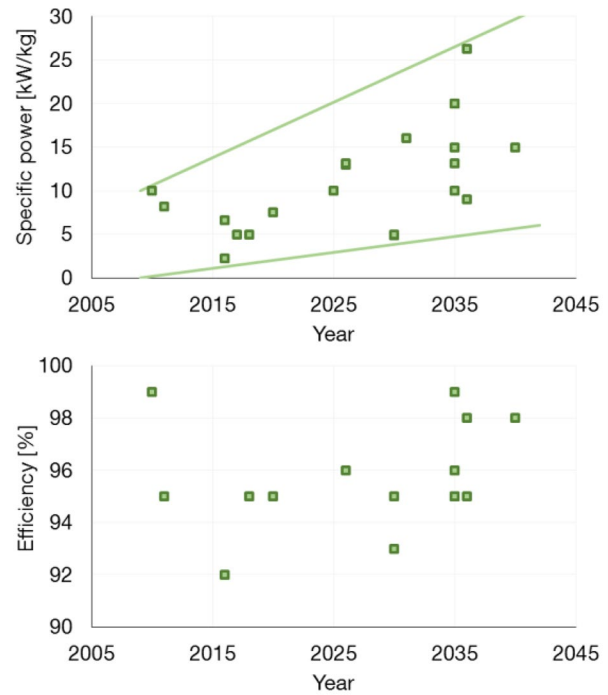
which is in turn transformed into thrust by the electric ducted fan (see Sect. 2.1.7).

As with the power transmission, non-superconducting electric motors are once again chosen in this study as the reference technology. Common designs of non-superconducting, conventional motors include synchronous, asynchronous and switched reluctance motors. State-of-the-art conventional electric motors achieve continuous specific powers of about 5 kW/kg and efficiencies of $92 - 98\%$ [40, 41]. A review of the relevant literature has been undertaken to compare predictions of the development of electric machine technology within other aircraft design-related studies. The results are shown in Fig. 7.

Assumptions for the specific power as high as 26. kW/kg [26] and efficiency predictions of up to 99% [10] have been found. A general upward trend can be identified for the specific power, as was expected. The efficiency data is more scattered however, but an increase of predictions can be observed towards 2035. For this study, values of 15 kW/kg and 95% are used in accordance with the shown data.

2.1.6 Gearbox sizing

A gearbox might be required to drive the electric ducted fan and account for the different rotational speeds of the electric motor and the electric ducted fan. As pointed out in [43], the mass of the electric motor sized for a (fixed) maximum

power demand is lower if the motor has a greater rotational speed. Hence, a gearbox is very likely required. It is modelled using the methods of ([44], Fig. 10) for efficiency and [45] for mass. As the electric motor model used in this study does not cover rotational speed calculations, the same gear ratio (2) as in the study of [43], which includes a more detailed motor model, is chosen in a first approximation.

2.1.7 Electric ducted fan sizing

As described before, the electric ducted fan converts the rotational mechanical power provided by the electric motor into thrust. The zero-dimensional thermodynamic performance model used in [11, 43] as developed by [46] is used to design the electric ducted fan and model its performance. The model is based on standard compressor theory and compressible flow relationships. These characterize stations along the electric ducted fan with static and stagnation temperatures, pressures and densities, mass flow, cross-sectional area and Mach number. The following assumptions have been made (Table 1):

The off-design behaviour of the electric ducted fan is predicted using the fan map from [47] as collected and edited by Kurzke for the program GasTurb [48], which is scaled to the actual fan design. The respective mass flow, rotational speed, thrust, efficiency and shaft power is then determined for each off-design point.

Table 1 Electric ducted fan sizing assumptions

Variable	Value
Design fan pressure ratio	1.4[a]
Design polytropic efficiency	90%
Fan face Mach number	0.6[a]
Hub-to-tip diameter ratio	0.3[a]
Length-to-diameter ratio	1.3[b]

[a]From ([43], Sect. 4.1.2). [b]From ([11], Fig. 3.11)
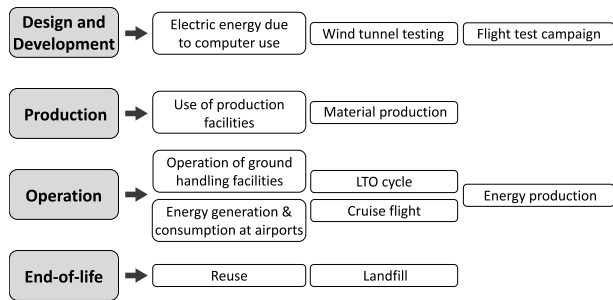
Fig. 8 Aircraft life cycle processes incorporated in the model, adopted from ([50], Fig. 3.3)

The mass of the electric ducted fan is estimated using the component built-up method as described in [49]. Its nacelle and pylon mass is computed using the same method as for the turbofan engines, as presented in [15].

2.2 Environmental life cycle analysis model

To be able to estimate and compare the environmental impact of existing and future aircraft concepts, a comprehensive and robust environmental LCA model that can be integrated in the aircraft design process is required. Such a methodology has been introduced, for example, by Johanning in [50]. It is taken as basis and further developed for the application to HEA in this study.

In general, all processes from the design and development to the end-of-life phase of an aircraft influence its environmental impact. The most relevant processes from each life cycle phase used in the inventory analysis by [50] are shown in Fig. 8. The ELCD database of the EU is consulted to undertake the inventory analysis for many of the considered processes. For more details on the data used in the inventory analysis, please refer to [50]. The ReCiPe 2008 method as described in [51] is used for the life cycle impact analysis. It is enhanced to consider the altitude-dependent effects of NO_X emissions and contrails based on the model of [52]. The inputs and outputs of each process resulting from the inventory analysis are normalized with the functional unit passenger-kilometer

(PKM) for better comparability. Based on the results of the inventory analysis, the impact of several midpoint (e.g., ozone depletion, terrestrial acidification, etc.) and three endpoint categories (damage to human health, ecosystem diversity and to resource availability) is calculated. The overall result is presented in the form of a single score (SS) summarizing the total environmental impact. It is important to note that the uncertainty levels rise from the midpoint categories up to the SS. To better deal with uncertainties, the ReCiPe method allows to account for different perspectives (options: *hierarchist*, *individualist*, *egalitarian*) and regions (options: *Europe* and *World*) grouping similar types of assumptions and choices. Different weighting perspectives with corresponding normalization factors are also available for the user to choose from (options: *average*, *hierarchist*, *individualist*, *egalitarian*). The *hierarchist* perspective combined with the *average* weighting option for the region *World* is used in the undertaken calculations. For a more complete description of the methodology, the reader is referred to [50, 51].

Besides the analysis of conventional, kerosene-powered aircraft, the environmental LCA model by Johanning also allows an analysis of all-electric aircraft and hydrogen-powered aircraft. This, in addition to its free online availability, is why it is chosen as a basis for this study. In order to make it applicable to HEA, the calculation methods for conventional and all-electric aircraft are combined as follows: the battery production process is incorporated in the production phase based on the total battery energy needed. In the operations phase, the in- and outputs from the kerosene production process are combined with those from the generation of electric energy to account for the total energy required for a flight. Since HEA require less fuel than conventional aircraft and also produce less combustion emissions due to the hybridization of the powertrain, these effects are directly incorporated by the trip fuel on board. It should be noted that due to the lack of precise knowledge regarding the exact composition of future batteries, a specific battery end-of-life scenario is not considered in the model. Additional adjustments to the model include the modification of some input parameters, such as the average load factor, to ensure that they are up-to-date, and the correction of the fuel burn calculation during the landing and take-off cycle to account for the number of jet engines.

To estimate the environmental impact of an HEA, the user is required to choose the configuration, the electric energy production method, the parameters of both power plants, the OEM, the fuel and battery mass, as well as the average mission range and flight altitude. The user obtains a complete analysis based on these inputs: life cycle inventory, impact on midpoint categories, impact on endpoint categories, and the total SS of the respective aircraft.

2.3 Direct operating costs model

The direct operating costs (DOC) estimation model used in this study is based on one of the most recent DOC methods. It has been developed at TU Berlin [53] and is implemented in the Central Reference Aircraft Data System (CeRAS) [54]. The reasons it was chosen as a basis for this study include the low number of required input parameters as well as the fact that it covers all relevant DOC elements such as ownership, maintenance, utilization and flight-related costs. In terms of results, a recent study of the DLR that compares various established DOC methods (among others the methods by ATA or AEA) has shown a good comparability of the different DOC element shares [55]. The absolute value of the calculated DOC does not over- or underestimate the DOC compared to the other models, but is located in a fairly average position. This makes the TU Berlin model a sensible choice.

However, since the TU Berlin model only considers current conventional transport aircraft technology, modifications accounting for HEA need to be included. Among others, these include the electricity price, capital costs for the batteries and maintenance costs for the electric powerplant. This work was done for regional hybrid-electric aircraft by Hoelzen et al., who modified the TU Berlin model and provided the respective equations in their paper [3]. Together with the original TU Berlin model for jet engine aircraft, this adaptation has been taken and altered so that it can be applied to commercial transport hybrid-electric aircraft.

Apart from adjusting some input parameters to better fit the aircraft segment under consideration (such as the number of battery sets required to cover the daily flights), an erratum in the equations provided by [3] was found. The equations have been revised accordingly after personal communication with J. Hoelzen (see the corrected equations in the "Appendix"). Furthermore, the maintenance costs calculation of the electric powertrain has been modified. As proposed in [25], they are estimated as a fraction of the costs of maintaining conventional engines. Kreimeier and Stumpf estimated this fraction from a study on electric cars [25] and found it to be 25%. However, in this study the DOC analysis on all-electric aircraft by Plötner et al. was consulted. They found that the powertrain maintenance costs of the all-electric aircraft were about 25% lower than those of a conventional reference aircraft ([56], Fig. 2). Hence, the fraction is 75%. Due to the uncertainty in estimating this fraction, the impact on the overall result is investigated in a parameter study (see "Appendix").

Having undertaken the adjustments to make the model applicable to HEA, some input parameters like fuel and electricity price were also updated. They are summarized in Table 2 and used for the baseline scenario analysis. The fuel price has been determined by averaging the jet fuel

Table 2 DOC model assumptions and their respective sources (baseline scenario)

Variable	Value	Source
Fuel price	80.13 $_{2019}$/bbl	[57]
Fuel price escalation	2.0%p.a.	[56]
Electricity price	0.12 €_{2019}/kWh	[67]
Electricity price escalation	1% p.a.	[56]
Battery charging efficiency	90%	[58]
Battery price	220 $_{2017}$/kWh	[62]
Battery price reduction	8%p.a.	[21, 62]
Battery residual value	40%	[3]
Battery cycles	1500	([21], p. 55)
Elec. powertr. maint. factor	0.75	([56], Fig. 2)
EM price	174 $_{2019}$/hp	[66]
Labour rate	50 €_{2019}/h	[53]
Unit cost rate noise	2.82 €_{2020}/noise unit	[68]
Unit cost rate NO_x	3.70 €_{2020}/kg	See text
CO_2 allowance price	15.48 €_{2018}/t	[69]
Portion auct. emission cert.	0.15	[70]
Clim. sens. area dist. factor	0	–
Unit cost rate climate toll	0.5 $_{2019}$/km	–

price as recorded by IATA between February 2019 and 2020 [57]. The mean value for the second half of 2019 for non-household consumers in the EU28 countries of 0.12 €/kWh has been taken for the electricity price. To account for electric energy losses during battery charging, a charging efficiency factor is introduced. It is based on a recent ADAC study investigating the charging efficiencies of electric cars [58]. The chosen 90% can be achieved with today's state-of-the-art, and thus represent a realistic value. A percentage increase of the fuel and electricity prices has been implemented: in the literature, the projection values for the future fuel price fluctuate between 1.3 and 2.26% p.a. [53, 56, 59, 60] and those for the future electricity price between 0 and 1% p.a. [56, 61]. The battery price is obtained from the cost of a battery pack in 2017 for electric cars ([62], Fig. 3). Considering the anticipated advancements in the field, a battery pack price reduction is implemented based on the average projections in [21, 62]. The battery residual value is somewhat difficult to estimate, as it depends largely on the battery usage. Thus, the value according to [3] has been adopted. However, the impact of this choice is examined in a parameter study (see "Appendix" and Sect. 4.2). As for the number of battery cycles, the high, but still realistic, value of 1500 for 2035 is taken as projected in ([21], p. 55). Values for the labour rate vary in literature between 40 $/h and 69 $/h [63–66]. Hence, the value of 50 €/h as suggested in the original DOC method was deemed adequate. Nevertheless, the influence of this value on the overall DOC is analyzed in a parameter study (see "Appendix" and Sect. 4.2).

In addition to the changes made to enhance the model for HEA, an inflation correction based on the corresponding GDP inflation factors from the years 2002 to 2035 (historical values and OECD forecast for Europe) [71] is added. Thereby, the DOC results can be provided for a user selected year. As the HEA are designed for an EIS of 2035, this year has been chosen as the evaluation year of the DOC.

Furthermore, to establish a meaningful comparison of conventional and hybrid-electric aircraft, environmental charging schemes are incorporated into the model. They account for noise and CO_2 & NO_X emission mitigation costs, which are increasingly being considered at airports around the world. The noise charges C_{noise} are estimated according to the recommended charging scheme proposed in [72], which is currently employed at all commercial Swedish airports.

$$C_{noise} = U_{noise} \cdot (10^{\frac{L_a - T_a}{10}} + 10^{\frac{L_d - T_d}{10}}) \tag{5}$$

where U_{noise} represents the unit noise charge, L_a and L_d the ICAO-certified noise levels for arrival and departure (average of sideline and take-off values), and T_a and T_d are the corresponding threshold values for both aircraft movements. Due to the lack of precise knowledge of the acoustic behaviour of the designed concepts, calculations of the L_a and L_d values are difficult. They have therefore been based on the results of a comprehensive acoustic analysis of Boeing's SUGAR Volt hybrid-electric aircraft ([23], Fig. 2.30), although the design Mach numbers of the Boeing concepts are lower. The noise fees showed a negligible impact of $\ll 1\%$ of the total DOC, therefore this assumption is deemed acceptable.

The ERLIG model is used to calculate the NO_X emission-related charges C_{NO_X} [73]. An analysis of the emissions charging schemes used has shown that the majority of European airports use the ERLIG model to levy NO_X emission-related charges.

$$C_{NO_X} = U_{NO_X} \cdot m_{NO_X,LTO} \tag{6}$$

The calculation includes the unit charge rate U_{NO_X} and the aircraft specific $m_{NO_X,LTO}$ emission value. The latter is based on the number of engines, fuel flow, and emissions during the standard landing and take-off (LTO) cycle. This information is obtained from the ICAO Aircraft Engine Emissions Databank. The former is taken as the average charge rate at large ($> 1m$ passengers) airports in Germany, Switzerland, Denmark, and Sweden that use the ERLIG method.

In Europe, commercial aviation is included in the Emissions Trading Scheme (ETS) of the EU and airlines are obliged to auction part of their CO_2 allowances from the market. Thus, these costs (C_{ETS}) are included in the model as well. They are the product of the CO_2 allowance price (U_{ETS}), the produced mass of CO_2 emissions due to kerosene burnt during the flight ($m_{CO_2,flight}$), and the portion of free allocated emission certificates (f_{ETS}).

$$C_{ETS} = U_{ETS} \cdot m_{CO_2,flight} \cdot (1 - f_{ETS}) \tag{7}$$

It is important to note that within this study, it is assumed that the aforementioned environmental charges, which are currently levied for the most part in Europe, are implemented on a global scale and not only in Europe or at certain airports.

Additionally, a climate toll charging system as proposed in [74] is implemented in the model in order to evaluate the monetary effect of future environmental impact mitigation activities. The formula's structure is based on the standard air navigation charge, where $U_{cl,toll}$ is the unit charge rate and k_1 and k_2 are country specific parameters. The degree of hybridization H is used to reduce the value of the toll charge ($C_{cl,toll}$) as an incentive for the employment of more environmentally-friendly technologies. The factor $f_{cl,toll}$ indicates the portion of the distance R flown in a climate sensitive area. It is determined by whether an airline decides to carry out its operations in a more climate optimal or cost optimal manner.

$$C_{cl,toll} = U_{cl,toll} \cdot \left(\frac{MTOM}{k_1}\right)^{k_2} \cdot (1 - H) \cdot R \cdot f_{cl,toll} \tag{8}$$

Although this additional charging system is not considered in the baseline case, it is included in the total DOC calculation for the investigated future scenario described in Sect. 4.3.

3 Use case: hybrid-electric, single-aisle aircraft

A comparison between a conventional aircraft and a hybrid-electric aircraft is undertaken as a use case for the previously described methodology. Both aircraft selected are single-aisle transport aircraft (A320 and B737 category). For reasons of comparison, both aircraft will be sized for the same requirements.

Due to the weight and volume of the batteries, the reasonable and feasible design ranges of the HEA are within 900–1700 nmi, as reported in previous studies [2, 4, 11, 29]. Block fuel reductions compared to a conventional reference aircraft have been presented for ranges below 900 nmi ([2], Fig. 9) and 1300 nmi ([75], Fig. 18) for comparable battery specific weights and energy densities as well as degrees of hybridization. Volumetric restrictions for design ranges above 1100 nmi (assuming a battery energy density of 1000 Wh/l) have been described in [76].

Bearing this information in mind, and analyzing the market of intraregional flights, a design range of 1000 nmi is

Table 3 Key specifications of the CRA and the HEA1000

Parameter	CRA	HEA1000	Δ
MTOM [kg]	60,174	85,077	+41.4%
OEM [kg]	36,443	44,587	+22.3%
Fuel mass[a] [kg]	5751	5377	−6.5%
Battery mass[a] [kg]	n/a	17,133	n/a
Energy[a] [kWh]	69,012	81,657	+18.3%
Payload mass [kg]	17,980	17,980	0%
Wing span [m]	34.2	42.6	+24.4%
Wing area [m^2]	93.7	144.9	+54.6%
Wing aspect ratio [-]	12.5	12.5	0%
L/D (initial cruise) [-]	18.6	20.3	+8.9%
Design range [nmi]	1000	1000	0%
Cruise Mach number [-]	0.78	0.78	0%

[a]Block and reserves

chosen for both the CRA and the HEA in this study. Iwanizki et al. found that more than about 85% of all intraregional flights within Europe, Africa and Asia & Oceania are operated below this range ([77], Fig.2) (based on OAG 2008 data). Hornung et al. concluded from their market study for 2035 that a range of 1000 nmi would cover 83% of all flights of aircraft within the 180-200 seats category ([78], Fig.2) (based on OAG 2010 data and air traffic growth factors). While this design range is thus a reasonable choice from a market analysis perspective, it should not be disregarded that it implies a reduction in operational flexibility for the airlines [2].

A CRA and an HEA with a battery specific energy of 1000 Wh/kg (in the following called HEA1000) are designed for this design range, a similar wing loading during landing, and based on the assumptions described in Sect. 2.1. Their essential specifications are provided in Table 3.

It can be seen that the HEA1000 has a 41.4% heavier MTOM which is the result of the carried battery mass of 17,133 kg, mass of other components of the electric powertrain, and related snowball effects. Despite the higher efficiency of the electric powertrain (compared to the conventional powertrain), the overall consumed energy of the HEA1000 is 18.3% greater compared to the CRA. The higher efficiency therefore does not outweigh the weight penalty. Furthermore, the wingspan increased substantially (24.4%), and is well beyond the 24–36 m of aircraft categorized under ICAO Code C. Even if the battery specific energy is taken as 1500 Wh/kg and only the mission segments take-off, climb, and cruise are flown hybridized, the resulting wingspan is 38.76 m for an MTOM of 71,602 kg. Here, of course, also the chosen aspect ratio needs to be considered.

The influence of individual flight phases on the fuel mass and electricity required is shown in Table 4.

Table 4 Trip energy breakdown of the CRA and the HEA1000

	CRA	HEA1000	
	Fuel [kg]	Fuel [kg]	Electricity [kWh]
Taxi	90	89	283
Take-off	72	71	226
Climb	1230	1218	3866
Cruise	2488	2209	6913
Descent & App.	405	411	1303
Landing	17	17	54

It can be seen that the most energy is required in the segments climb and cruise. For all mission segments except descent & approach and landing, the HEA1000 requires less fuel than the CRA, although it is heavier and its turbofan engines have a higher TSFC: The total sea-level static thrust of the CRA is 181.3 kN (two turbofans at 90.6 kN). For the HEA1000 it is 218 kN (two turbofans at 79.8 kN and two electric ducted fans at 29.3 kN). The larger turbofans of the CRA have a lower TSFC in initial cruise than those of the HEA1000 ($1.33 \ 10^{-5}$ and $1.35 \ 10^{-5}$ $kg/(sN)$, respectively), accounting for the size effects of smaller gas turbines. The higher required energy for descent & approach and landing[2] might be attributed to the greater landing weight of the HEA1000, since the batteries have to be carried along the full mission.

The required electricity in kWh can be interpreted as battery mass required per mission segment as the specific energy of the batteries is 1 kWh/kg. Especially in comparison with the required fuel mass, it becomes evident how heavy the battery needs to be for a degree of hybridization of 0.3 only. Adding battery (fuel) mass for loiter, diversion, and contingency, leads to the block battery (fuel) mass stated in Table 3.

Unfortunately, the design of HEA involves many different assumptions (e.g., powertrain architecture, operating strategy, degree of hybridization, component technology assumptions, clean-sheet or retro-fit design,...), which are often not provided to enable the reproduction of the results of these publications. Therefore, a direct comparison of the results with other publications is difficult. Nonetheless, two studies on single-aisle HEA of a similar class have been identified which were similar enough as to compare with this study:

– Pornet conducted a clean-sheet design of a discrete parallel HEA for a design range of 1300 nmi, a bat-

---

[2] The identical numerical values of required fuel for landing can be attributed to rounding differences.

Table 5 Comparison of results with study of Pornet

	Pornet ([11], Table 5.8)	ADEBO
MTOM [kg]	77, 730	79, 130
OEM [kg]	41, 818	42, 844
Fuel mass [kg]	5806	6539
Battery mass [kg]	11, 740	11, 447

**Table 6** Comparison of results with study of Aigner et al

	Aigner et al. ([2], p. 11)	ADEBO
MTOM [kg]	73, 000	76, 829
OEM [kg]	45, 900	41, 499
Fuel mass [kg]	7300	4945
Battery mass [kg]	5100	15, 766

tery specific energy of 1500 Wh/kg at cell level, and a payload mass of 18,360 kg. A calculation for similar assumptions with the HEA design methodology of this paper, resulted in the data provided in Table 5. Although some differences exist and can be attributed to different modelling assumptions, the order of magnitude of the data is the same.

- Aigner et al. also undertook the conceptual design of a discrete parallel HEA with a range of 1000 nmi, a battery specific energy of 1000 Wh/kg, and a payload mass of ca. 14.6 t. Unfortunately, no further design specifications (like e.g., wing aspect ratio, turbofan fuel efficiency, hybridized mission segments, etc.) are given, such that a comparative calculation is difficult. Assuming that all mission segments are hybridized, an aspect ratio of 12.5 and a TSFC of the turbofans of the HEA of $1.35 \, 10^{-5}$ kg/(sN), results within ADEBO are calculated (see Table 6). A large deviation, especially of the battery mass (factor of 3), and also the fuel mass, is found. Most probably, the underlying assumptions of Aigner et al.'s study are different, which unfortunately could not be verified.

4 Results and discussion

In this section the results of the application of the established methodology are presented. It is subdivided in three parts: (1) a comparison of the CRA and HEA1000 in terms of the SS and the DOC for the baseline scenario,
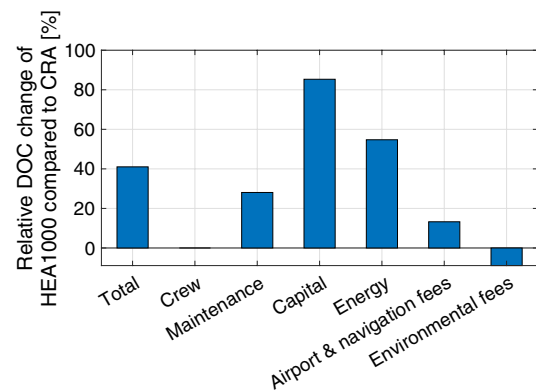
Fig. 9 Relative change of DOC components of HEA1000 compared to CRA (baseline scenario)

(2) the parameter studies, and (3) the comparison of the CRA and the HEA1000 for a fictional future scenario.

4.1 Comparison of CRA and HEA1000 (baseline scenario)

Both the designed CRA and the HEA1000 have been evaluated with respect to their DOC and SS. Figure 9 shows the relative changes to the DOC components crew, maintenance, capital, energy, and fee.

A total increase of the DOC of about 41.0% is observed, the greatest increase being in the capital costs. This is due to the additional capital costs of the battery. As expected, the crew costs remain constant. The maintenance costs increase because of the higher OEM and the additional electric powertrain of the HEA1000. Additionally, the energy (kerosene and electricity) costs increase by 54.7%. On the one hand this can be attributed to the increased energy required by the HEA for the same mission (see Table 3), but also to the difference in costs per kWh for kerosene and electricity (in these terms, electric energy is more expensive by a factor of more than two). As airport and navigation fees are proportional to the MTOM, they also increase for the HEA1000. Environmental fees, however, are reduced by 8.9%, which can be attributed to a lower fuel burn and thus lower $m_{CO_2,\text{flight}}$, and a lower $m_{NO_x,\text{LTO}}$ of the HEA.

The relative DOC shares of the CRA and the HEA1000 are compared in Fig. 10. It can be observed that the relative significance of the total capital and energy costs increases, and of the fees decreases, as expected. Although the absolute value of the maintenance costs increases, its DOC share remains about constant. And while the absolute crew costs remain constant, their relative share decreases.

Isikveren et al. evaluated the operating costs of an HEA of similar size (single-aisle, 180 passengers) and architecture (discrete parallel). However, they only considered the cash operating costs and environmental charges (leaving out
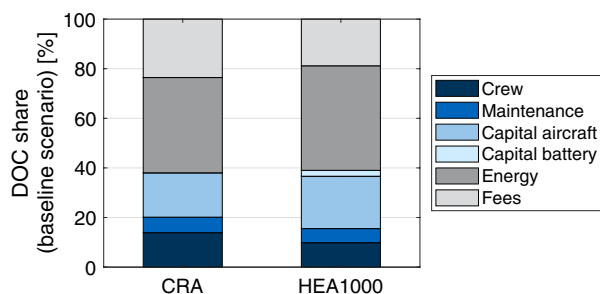
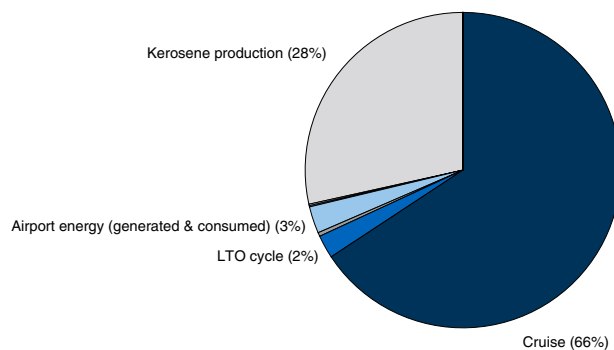Fig. 10 Comparison of DOC shares of CRA and HEA1000 (baseline scenario)
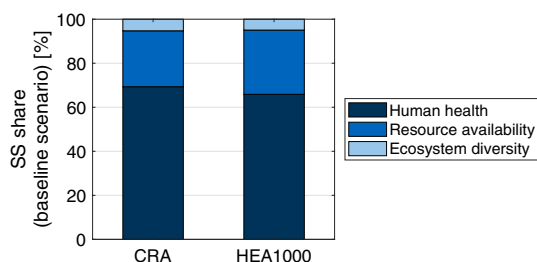
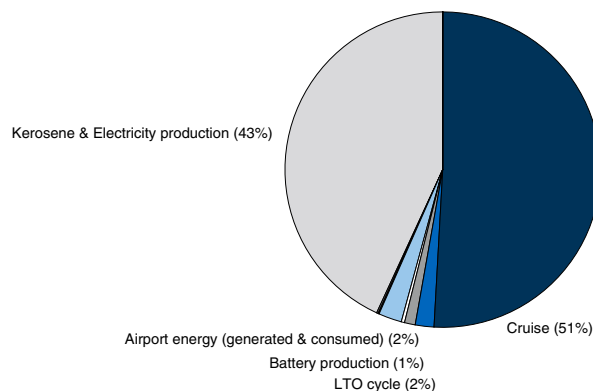Fig. 11 Comparison of SS shares of endpoint categories for CRA and HEA1000 (baseline scenario)

(a) CRA

(b) HEA1000

Fig. 12 Comparison of SS shares of processes of CRA (**a**) and HEA1000 (**b**) (baseline scenario). For better readability, only processes with a share ≥ 1% are labelled

the capital costs). They found that the costs of the HEA compared to the conventional reference aircraft increased by 10.9% ([6], Table 1). This value has been calculated within this study as well, and was found to be 31.4%. However, a direct comparison of both values is difficult, as the degree of hybridization (and thus, the amount of electric energy required) in Isikveren et al. is different to the one chosen in this study. Since energy cost have a large share on cash operating cost, the costs depend highly on the assumptions for degree of hybridization, fuel cost, and electricity cost. Nevertheless, the general tendency of HEA being more expensive to operate is the same for both studies.

The environmental life cycle analysis results yield a SS of 0.011125 points/PKM (CRA) and 0.012805 points/PKM (HEA1000). This equates to a 15.1% increase of environmental impact of the HEA1000 compared to the CRA. Even with improved battery technology (1500 Wh/kg), the relative SS of the HEA remains 3.2% greater. Additionally, a shift in endpoint category relative importance towards resource availability can be seen (Fig. 11). This can be attributed to the copper ore, natural gas, crude oil, brown coal, and hard coal resources needed for electricity and battery production, among others.

The absolute SS and the SS shares of the CRA (69.3%, 25.4%, and 5.3%) are comparable to the results for the A320-200 presented by Johanning of 0.0176 points/PKM and shares of 69%, 26% and 5% for human health, resource availability and ecosystem diversity, respectively ([50], Table 3.29 & Fig. 3.11). The greater absolute SS can

possibly be attributed to the longer range (factor 1.5) and thus higher fuel burn of the A320-200. The most relevant life cycle phase is the operation of the aircraft: for the CRA, this phase makes up 97.3% and for the HEA1000 96.6% of the SS share. This result is in-line with the findings of other aircraft environmental LCA studies (see e.g., [50, 79–82]).

Figure 12 displays the SS shares the different processes make up for the CRA (a) and the HEA1000 (b).

A clear shift from cruise to energy carrier production can be observed: 66% (cruise) and 28% (kerosene production) for the CRA, while 51% (cruise) and 43% (kerosene and electricity production) for the HEA1000. This result is in-line with the findings of Johanning for the analyzed all-electric aircraft, and also for the investigated H_2 aircraft, and the aircraft powered with alternative fuel ([50], p. 116). Battery production, however, only contributes about 1% to the total SS of the HEA1000.

4.2 Parametric studies

As discussed above, some inputs of the direct operating costs model are subject to great uncertainties (e.g., the battery
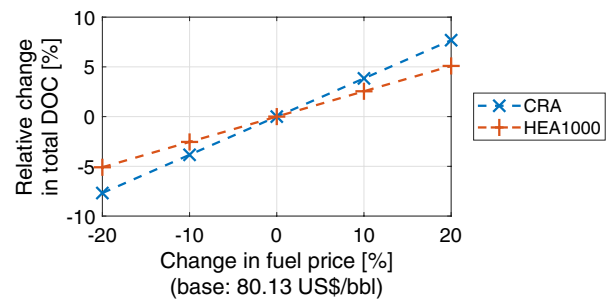
(a) Total DOC
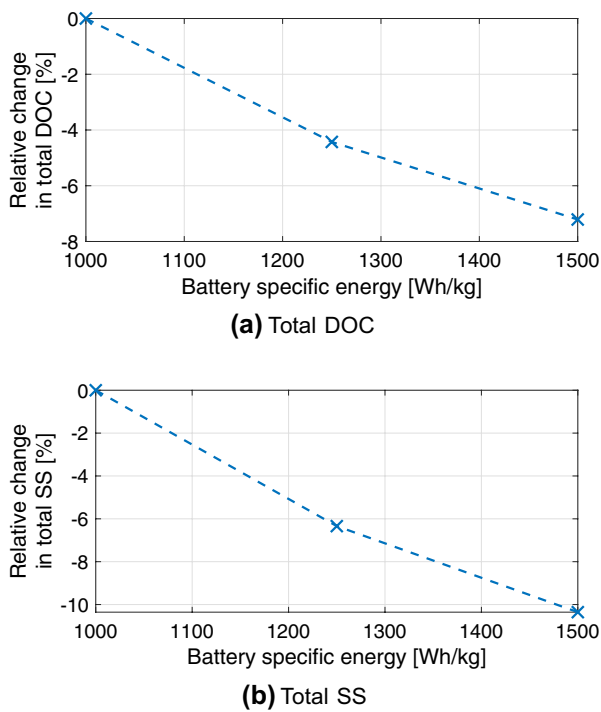
(b) Total SS

Fig. 13 Parameter studies of different battery specific energy levels affecting the total DOC (**a**) and total SS (**b**) of the HEA
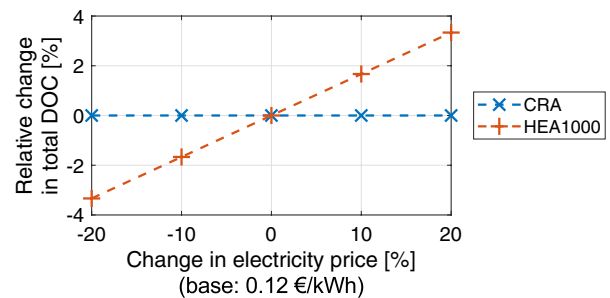

Fig. 14 Influence of the fuel price on the total DOC (baseline scenario)

Fig. 15 Influence of the electricity price on the total DOC (baseline scenario)

residual value and the electric powertrain maintenance factor). Parameter studies for these values were conducted to analyze the potential impact on the results. Furthermore, additional parameter studies were undertaken to identify the main drivers of the DOC and SS results.

The results of the parameter studies show that the impact of a $\pm 20\%$ change in the battery residual value, the electric powertrain maintenance factor, and the labour rate leads to a linear response and a relative change in total DOC below $\pm 0.3\%$ (see Fig. 19, 20 and 21 in the "Appendix"). Due to the minor influence on the overall results, the assumed values are considered acceptable.

One of the main drivers for the design of HEA has been identified as the battery specific energy, since it directly affects the battery mass and thus the MTOM of the aircraft. Different HEA configurations are therefore evaluated in terms of their battery specific energy. The corresponding influence on the total direct operating costs and environmental impact is compared in Fig. 13. Due to the high impact of the battery specific energy on the aircraft mass, the employment of a more technologically improved battery results in lower DOC, as expected. A relative reduction of -7.2% in total DOC is achieved if 1500 Wh/kg batteries are used. In terms of the environmental impact of the different configurations, a lighter aircraft resulting from the use of batteries with a higher specific energy requires less energy (kerosene and electric energy) to complete its mission and

consequently produces fewer emissions. This trend is visualized by the -6.3% and -10.4% relative reduction in total SS for the 1250 Wh/kg and 1500 Wh/kg batteries. The kink in both curves can be attributed to the fact that the hybrid-electric aircraft design is not a linear process, but involves snowball effects. The HEA1000 has a battery mass (block and reserves) to OEM fraction of 38.4%. The other two HEA derivatives with 1250 Wh/kg and 1500 Wh/kg have lower fractions of 30.2% and 24.8%. As such, the decreasing fraction makes sense (the battery is lighter for the same amount of energy stored), but also illustrates the non-linear behaviour of the resulting aircraft design. This is likely to be the reason for the similar curve shapes of the DOC and SS changes.

The influence on the total DOC of the change in fuel price for the baseline scenario is displayed in Fig. 14. Due to the larger portion of fuel required to operate the CRA, its total DOC show a larger dependency on the fuel price compared to the HEA1000. The steeper slope of the relative DOC change curve for the CRA illustrates this dependency.

Figure 15 depicts the relative change in total DOC as a result of varying the electricity price. A relative total DOC change of around $\pm 3.3\%$ is obtained for an electricity price variation ranging from $\pm 20\%$ from the base value for the HEA1000. Since the CRA is powered only by conventional gas turbine engines, its DOC are not affected by changes in the electricity price, resulting in the flat blue curve.
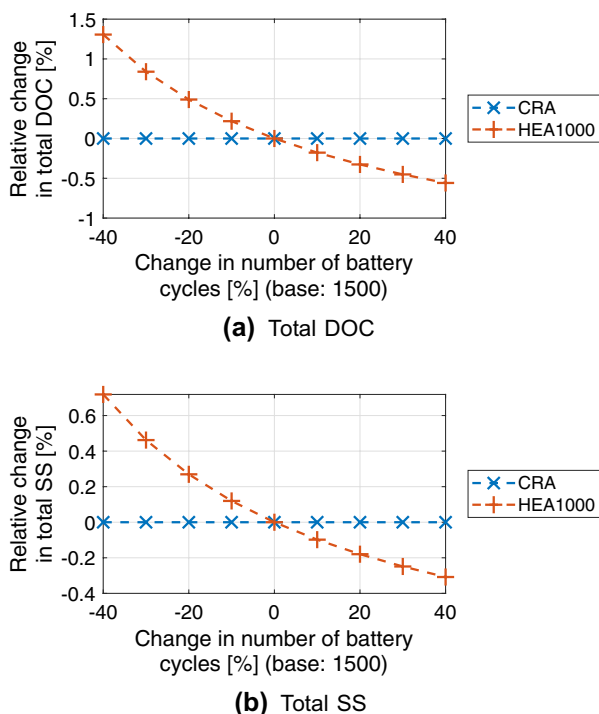
Fig. 16 Parameter studies for different number of battery cycles influencing the total DOC (**a**) and total SS (**b**)

Considering the relatively large share of the energy costs component for the DOC compared to the rest, and the aforementioned influences of the kerosene and electricity price on the total DOC, the energy price levels can be identified as one of the main cost driving factors for HEA.

Another interesting observation is the influence of the number of battery cycles of a single battery pack before it has to be replaced. Figure 16 displays the non-linear, relative change in total DOC (a) and total SS (b) arising from an increase/decrease in the battery operating cycles. The number of battery cycles directly influences the battery depreciation and thus the battery annuity rate. Thus, an increase in DOC resulting from a shorter battery life (lower number of battery cycles) can be expected. A shorter battery life affects the aircraft's environmental impact as well, due to the increased number of battery packs that need to be produced. As the CRA does not use batteries, there is no dependency regarding the number of battery cycles.

The results of further parameter studies can be found in the "Appendix".

4.3 Comparison of CRA and HEA1000 (future scenario)

In addition to the baseline scenario, the DOC and SS of the CRA and HEA1000 have also been evaluated for a fictional future scenario. Following the trend of increasing

Table 7 DOC model assumptions (future scenario) - only altered values shown

| Variable	Value
Fuel price	90 $_{2019}$//bbl
Electricity price	0.10 €$_{2019}$/kWh
Battery charging efficiency	95%
Battery price reduction	10%p.a.
Battery cycles	2000
Elec. powertrain maint. factor	0.6
Unit cost rate noise	5.65 €$_{2020}$/noise unit
Unit cost rate NO$_x$	18.96 €$_{2020}$/kg
CO$_2$ allowance price	20.00 €$_{2018}$/t
Portion of auct. emission cert.	0.5
Climate sensitive area dist. factor	0.25
Unit cost rate climate toll	3 $_{2019}$/km
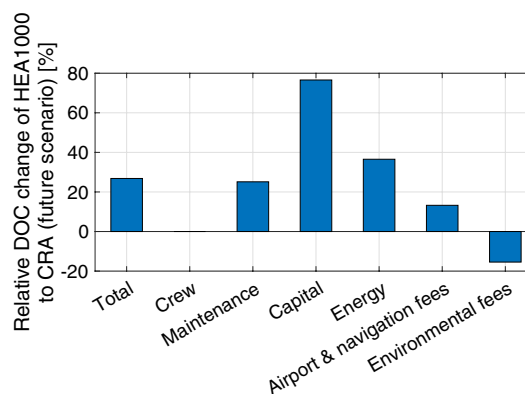
Fig. 17 Relative change of DOC components for HEA1000 compared to CRA (future scenario)

global environmental awareness, more stringent noise and emissions charges as well as a higher portion of auctioned CO$_2$ allowances have been considered. A unit cost rate of 3 $_{2019}$/km for the newly introduced climate toll charge is adopted. Climate-optimal flying would always be less expensive than business as usual for values above this threshold according to the findings of Niklaß in ([74], p. 106). Furthermore, in order to maximize the environmental reduction potential of HEA, only electric energy produced from renewable sources is considered for this scenario, as concluded by other studies (e.g., [3–5]). Table 7 summarizes the assumptions made for the future scenario.

Based on these assumptions, a total increase in the DOC of around 26.8% is obtained for the HEA1000 configuration compared to the CRA (see Fig. 17). As in the baseline scenario, an increase in the DOC components maintenance, capital, energy, and airport & navigation fees is observed for the HEA1000. However, it is more moderate in this scenario. Regarding the energy costs, the rise in fuel price is offset by the reduced electricity price in combination with the higher battery charging
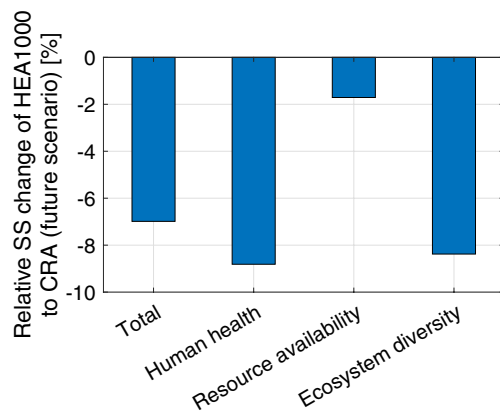
Fig. 18 Relative change of SS endpoint categories of HEA1000 compared to CRA (future scenario)

Table 8 Relative comparison of DOC and SS of HEA1000 vs. CRA

	DOC	SS
Baseline scenario	+41.0%	+15.1%
Future scenario	+26.8%	−7.0%

efficiency. Although a longer battery life and a higher yearly battery price reduction are assumed in this scenario, the relative capital costs change of the HEA1000 compared to the CRA remain over 75%. A DOC advantage of the HEA1000 can be seen in the environmental fees component. Main drivers here are the more stringent emission charges and higher ETS expenses as well as the inclusion of the aforementioned climate toll. These contribute to the approximately −15.4% lower environmental fees for the HEA1000 compared to the CRA.

Figure 18 illustrates the relative changes of the total SS and the three endpoint categories for the HEA1000 compared to the CRA. The results of the environmental life cycle analysis show a relative reduction of the total SS for the HEA1000 of −7.0%. Compared to the baseline scenario, this represents an environmental benefit. That can also be seen in the relative decreases in each of the endpoint categories. An interesting observation can be made regarding the endpoint category resource availability. The HEA1000 has a lower impact on resource availability than the CRA for the future scenario, which was not the case in the baseline scenario. On the one hand, this can be attributed to the different form of electricity production – renewable instead of the current European electricity production mix. This finding is in line with the observations from other studies, e.g., [3–5]. On the other hand, a reduced number of batteries needs to be produced due to the 33.3% increase in battery lifetime (cycles) compared to the baseline scenario, leading to less use of copper ore, natural gas, crude oil, and hard coal. However, this increase in the battery lifetime has a small impact on the overall SS reduction (see Fig. 16b).

5 Conclusion and future work

In this study, a methodology to design and evaluate hybrid-electric, single-aisle transport aircraft with a discrete parallel powertrain architecture with respect to their direct operating costs and their life cycle environmental impact has been developed. Different scenarios and parameter studies have been calculated. By this the conditions under which HEA might be a viable option to reduce the climate impact of aviation have been determined. The main finding of the study is that the environmental impact of the HEA1000 configuration (discrete parallel powertrain architecture, battery specific energy of 1000 Wh/kg, degree of hybridization $H = 0.3$) was increased by 15.1% for a baseline scenario, while the operating costs increased by 41.0% compared to a conventional reference aircraft. For a future scenario, the environmental impact was reduced by 7.0% and the operating costs increase was lower. In this scenario the electricity is produced from renewable sources, the battery lifetime is longer, the fuel price higher, the electricity price lower, and the environmental charges levied at airports and by authorities increased, among others. Table 8 summarizes the main findings of this study regarding the economic (DOC) and environmental (SS) evaluation of hybrid-electric, single-aisle transport aircraft.

Hence, it can be concluded that discrete parallel HEA are a potential solution to reduce the climate impact of the aviation industry when the electricity is produced from renewable sources. However, this comes at the expense of increased direct operating costs in both scenarios.

Future work associated with this study should comprise the improvement of the HEA design process with more detailed models, especially for the electric motor and the power electronics. Additionally to revising the HEA design process, the DOC model assumptions should also be refined. Special attention should hereby be paid to the certified noise levels of the HEA. Equally important is an update of the environmental LCA model to a new database and to the completely revised ReCiPe 2016 method to include recent developments in the fields of life cycle inventory and impact assessment.

The next steps then include the optimization of an HEA design for the SS and for the DOC, creating a Pareto front and establishing the trade-off for different degrees of hybridization. Here it would be particularly interesting to investigate the change in results when using alternative fuels in both the CRA and the HEA. The analysis would greatly benefit from being repeated for different future scenarios, different mission ranges, and being applied to different HEA architectures. One could also consider including the operating strategy of the HEA in the analysis. Furthermore,

benefits of using synergies offered by electric propulsion, such as e.g., distributed electric propulsion, should be explored. Aerodynamic performance improvements might alleviate the DOC penalty.

Appendix

A.1 DOC model supplementary information

Revised equations of [3] after personal communication with J. Hoelzen.

Equation A4 in [3]:

$$\mathrm{DOC_{Ma}} = \left(\mathrm{DOC_{AF,mat}} + \mathrm{DOC_{AF,per}} + \mathrm{DOC_{Eng}}\right) \cdot \mathrm{FC} + \mathrm{DOC_{Tec}} \tag{9}$$

Equation A13 in [3]:

$$\mathrm{DOC_{Cap,Bat}} = 3 \cdot E_{\mathrm{Bat}} \cdot p_{\mathrm{Bat}} \cdot \left(a_{\mathrm{Bat}} + f_{\mathrm{ins}}\right) \tag{10}$$

A.2 Further parameter study results

See Figs. 19, 20, 21, 22, 23, 24
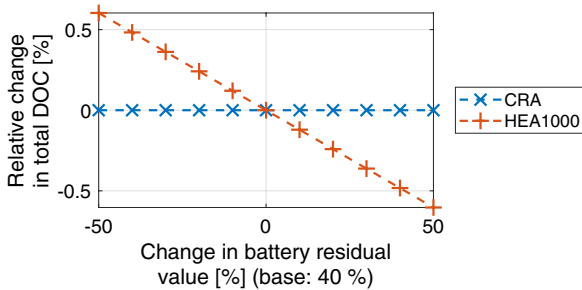
Fig. 19 Variation of the battery residual value
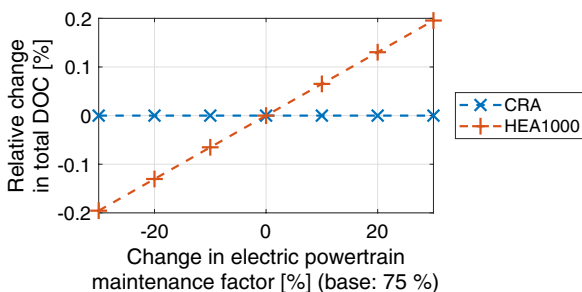
Fig. 20 Influence of the electric powertrain maintenance factor on the total DOC (baseline scenario)
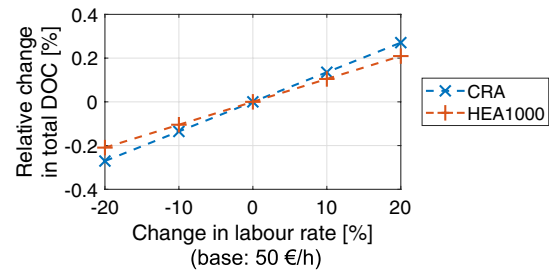
Fig. 21 Influence of the labour rate on the total DOC (baseline scenario)
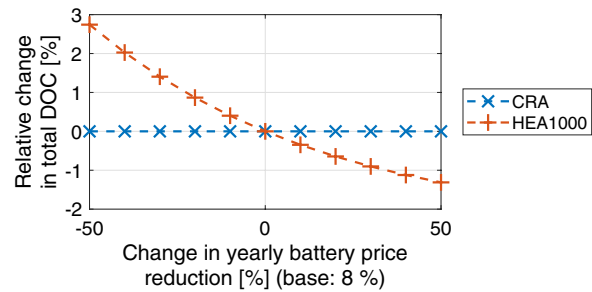
Fig. 22 Influence of the yearly battery price reduction on the total DOC (baseline scenario)
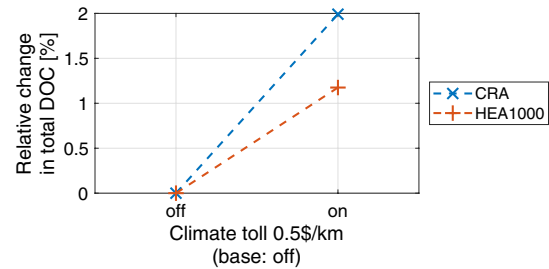

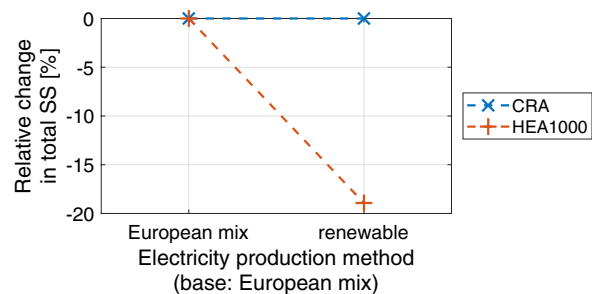**Fig. 23** Influence of the climate toll on the total DOC (baseline scenario)

Fig. 24 Influence of the electricity production method on the total SS (baseline scenario)

Declarations

Conflict of interest The authors declare that they have no conflict of interest.

References

1. Airbus Group: Global Market Forecast 2019-2038. https://www.airbus.com/aircraft/market/global-market-forecast.html [Accessed: 06/02/2020]

2. Aigner, B., Nollmann, M., Stumpf, E.: Design of a hybrid electric propulsion system within a preliminary aircraft design software environment, in Proc 67th Deutscher Luft- und Raumfahrtkongress. DGLR, Friedrichshafen (2018)

3. Hoelzen, J., Liu, Y., Bensmann, B., Winnefeld, C., Elham, A., Friedrichs, J., Hanke-Rauschenbach, R.: Conceptual design of operation strategies for hybrid electric aircraft. Energies **11**(1), 217 (2018)

4. Wroblewski, G.E., Ansell, P.J.: Mission analysis and emissions for conventional and hybrid-electric commercial transport aircraft, in Proc 2018 AIAA Aerospace Sciences Meeting. AIAA SciTech Forum, Kissimmee (2018)

5. Gesell, H., Wolters, F., Plohr, M.: System analysis of turbo electric and hybrid electric propulsion systems on a regional aircraft, in Proc 31st Congress of the International Council of the Aeronautical Sciences. ICAS, Belo Horizonte (2018)

6. Isikveren, A.T., Pornet, C., Vratny, P.C., Schmidt, M.: Conceptual studies of future hybrid-electric regional aircraft, in Proc 22nd International Symposium on Air Breathing Engines. ISABE, Phoenix (2015)

7. Herbst, S.: Development of an aircraft design environment using an object-oriented data model in MATLAB. Ph.D. thesis, Technical University of Munich, Munich (2018)

8. Drela, M., Youngren, H.: Athena Vortex Lattice 3.37 [Computer software], Cambridge. Massachusetts (2002)

9. National Academies of Sciences, Engineering, and Medicine: Commercial aircraft propulsion and energy systems research – reducing global carbon emissions. The National Academies Press. Washington D.C. (2016)

10. Kuhn, H., Seitz, A., Lorenz, L., Isikveren, A.T., Sizmann, A.: Progress and perspectives of electric air transport, in Proc 28th Congress of the International Council of the Aeronautical Sciences. ICAS, Brisbane (2012)

11. Pornet, C.: Conceptual design methods for sizing and performance of hybrid-electric transport aircraft. Ph.D. thesis, Technical University of Munich, Munich (2018)

12. Brelje, B.J., Martins, J.R.R.A.: Electric, hybrid, and turboelectric fixed-wing aircraft: a review of concepts, models, and design approaches. Prog. Aerosp. Sci. **104**, 1 (2019)

13. Roskam, J.: Airplane design: part I preliminary sizing of airplanes. Roskam Aviation and Engineering Corporation, Ottawa (1985)

14. Torenbeek, E.: Synthesis of subsonic airplane design. Delft University Press, Rotterdam (1976)

15. LTH Koordinierungsstelle: Luftfahrttechnisches Handbuch (LTH): Handbuch Masseanalyse. W. Sellner, Ingenieurbüro für Flugzeugtechnik, Höhenkirchen-Siegertsbrunn (2006). http://www.lth-online.de

16. Raymer, D.P.: Aircraft design: a conceptual approach, 6th edn. United States, AIAA Education Series American Institute of Aeronautics and Astronautics, Reston (2018)

17. Malone, B., Mason, W.H.: Multidisciplinary optimization in aircraft design using analytic technology models. J Aircraft **32**(2), 431 (1995)

18. Raymer, D.P.: Aircraft design: a conceptual approach, 5th edn. United States, AIAA Education Series American Institute of Aeronautics and Astronautics, Reston (2012)

19. Howe, D.: Aircraft conceptual design synthesis. Professional Engineering Publishing Limited, London (2000)

20. Druot, T.Y., Belleville, M., Roches, P., Gallard, F., Peteilh, N., Gazaix, A.: A multidisciplinary airplane research integrated library with applications to partial turboelectric propulsion, in Proc AIAA Aviation 2019 Forum. AIAA Aviation Forum, Dallas (2019)

21. Thielmann, A., Neef, C., Hettesheimer, T., Döscher, H., Wietschel, M., Tübke, J.: Energy storage roadmap [Energiespeicher Roadmap]. Tech. rep, Fraunhofer-Institut für System und Innovationsforschung ISI, Karlsruhe (2017)

22. CRC: Handbook of aviation fuel properties. Tech. Rep. No. 530, Coordinating Research Council, Inc, Atlanta (1983)

23. Bradley, M.K., Droney, C.K.: Subsonic ultra green aircraft research: phase II – volume II – hybrid electric design exploration. Tech. Rep. NASA CR-2015-218704, Boeing Research and Technology, Huntington Beach (2015)

24. Strack, M., Chiozzotto, G.P., Iwanizki, M., Plohr, M., Kuhn, M.: Conceptual design assessment of advanced hybrid electric turboprop aircraft configurations, in Proc 17th AIAA Aviation Technology, Integration, and Operations Conference. AIAA Aviation Forum, Denver (2017)

25. Kreimeier, M., Stumpf, E.: Benefit evaluation electric propulsion concepts for CS-23 aircraft. CEAS Aeronaut. J. **8**, 691 (2018)

26. Lents, C.E., Hardin, L.W., Rheaume, J., Kohlman, L.: Parallel hybrid gas-electric geared turbofan engine conceptual design and benefits analysis, in Proc 52nd AIAA/SAE/ASEE Joint Propulsion Conference. Propulsion and Energy Forum, Salt Lake City (2016)

27. Tan, S.C.: Electrically assisted propulsion & power systems for short-range missions. Master's thesis, Delft University of Technology, Delft (2018)

28. Girishkumar, G., McCloskey, B., Luntz, A.C., Swanson, S., Wilcke, W.: Lithium-air battery: promise and challenges. J. Phys. Chem. Lett. **1**(14), 2193 (2010)

29. Pornet, C., Gologan, C., Vratny, P.C., Seitz, A., Schmitz, O., Isikveren, A.T., Hornung, M.: Methodology for sizing and performance assessment of hybrid energy aircraft. J Aircraft **52**(1), 341 (2015)

30. Voskuijl, M., van Bogaert, J., Rao, A.: Analysis and design of hybrid electric regional turboprop aircraft. CEAS Aeronaut. J. **9**, 15 (2018)

31. Madonna, V., Giangrande, P., Galea, M.: Electrical power generation in aircraft: review, challenges, and opportunities. IEEE T Transp. Electr. **4**(3), 646 (2018)

32. Isikveren, A.T., Seitz, A., Vratny, P.C., Pornet, C., Plötner, K.O., Hornung, M.: Conceptual studies of universally-electric systems architectures suitable for transport aircraft, in Proc 61st Deutscher Luft- und Raumfahrtkongress. DGLR, Berlin (2012)

33. Vratny, P.C., Kuhn, H., Hornung, M.: Influences of voltage variations on electric power architectures for hybrid energy aircraft, in Proc 64th Deutscher Luft- und Raumfahrtkongress. DGLR, Rostock (2015)

34. Stückl, S., van Toor, J., Lobentanzer, H.: Voltair – the all electric propulsion concept platform – a vision for atmospheric friendly flight, in Proc 28th Congress of the International Council of the Aeronautical Sciences. ICAS, Brisbane (2012)

35. Stückl, S.: Methods for the design and evaluation of future aircraft concepts utilizing electric propulsion systems. Ph.D. thesis, Technical University of Munich, Munich (2016)

36. Borealis AG: Case Study: HEP ODS chooses XLPE insulation to ensure reliable power supply in Croatia (2019)

37. Andrea, J., Buffo, M., Guillard, E., Landfried, R., Boukadoum, R., Teste, P.: Arcing fault in aircraft distribution network, in Proc 2017 IEEE Holm Conference on Electrical Contacts, pp. 317–324. IEEE, Denver (2017)

38. Boukadoum, R., Landfried, R., Leblanc, T., Teste, P., Andrea, J.: Role of the pressure in the DC electric arc characteristics application: case of the more electrical aircraft, in Proc 28th International Conference on Electric Contacts ICEC 2016. IEEE, Edinburgh (2016)

39. Welstead, J., Felder, J.L.: Conceptual design of a single-aisle turboelectric commercial transport with fuselage boundary layer ingestion, in Proc 54th AIAA Aerospace Sciences Meeting. AIAA Scitech Forum, San Diego (2016)

40. Siemens AG: Factsheet – Rekord-Motor SP260D und Extra 330LE (2015)

41. Emrax d.o.o.: EMRAX 268 technical data table (dynamometer test data) (2018)

42. Vratny, P.C.: Conceptual design of an all-electric regional aircraft powered by battery. Master's thesis, University of Applied Sciences FH Joanneum, Graz (2011)

43. Vratny, P.C.: Conceptual design methods of electric power architectures for hybrid energy aircraft. Ph.D. thesis, Technical University of Munich, Munich (2018)

44. Anderson, N.E., Loewenthal, S.H., Black, J.D.: An analytical method to predict efficiency of aircraft gearboxes. Tech. Rep. NASA 84-C-8, Lewis Research Center, Cleveland (1984)

45. Brown, G.V., Kascak, A.F., Ebihara, B., Johnson, D., Choi, B., Siebert, M., Buccieri, C.: NASA Glenn research center program in high power density motors for aeropropulsion. Tech. Rep. NASA/TM-2005-213800, Glenn Research Center, Cleveland (2005)

46. Steiner, H.-J. and Schmitz, O.: Ducted Fan Model. Internal Report No. IB-11013, Bauhaus Luftfahrt e.V., Munich (2011)

47. Freeman, C., Cumpsty, N.A.: Method for the prediction of supersonic compressor blade performance. J. Propul. Power. **8**(1), (1992)

48. Kurzke, J.: GasTurb 11 Laboratory [Computer software] (2007)

49. Onat, E., Klees, G.W.: A method to estimate weight and dimensions of large and small gas turbine engines. Tech. Rep. NASA-CR199481, Boeing Military Airplane Development, Seattle (1979)

50. Johanning, A.: A method for the environmental life cycle analysis during conceptual aircraft design [Methodik zur Ökobilanzierung im Flugzeugvorentwurf]. Ph.D. thesis, Technical University of Munich, Munich (2017)

51. Goedkoop, M., Heijungs, R., Huijbregts, M., De Schryver, A., Struijs, J., Van Zelm, R.: Recipe 2008: A life cycle impact assessment method which comprises harmonised category indicators at the midpoint and the endpoint level. Characterisation. Tech. rep., Ministerie van Volkshuisvesting, Ruimtelijke Ordening en Milieubeheer, Report I (2009)

52. Schwartz Dallara, E.: Aircraft design for reduced climate impact. Ph.D. thesis, Stanford University, Stanford (2011)

53. Thorbeck, J., Scholz, D.: DOC-Assessment method (2013). [Presentation] 3rd Symposium on Collaboration in Aircraft Design, Linköping, Sweden. https://www.fzt.haw-hamburg.de/pers/Scholz/Aero/TU-Berlin_DOC-Method_with_remarks_13-09-19.pdf [Accessed: 22/07/2020]

54. Risse, K., Schäfer, K., Schültke, F., Stumpf, E.: Central reference aircraft data system (CeRAS) for research community. CEAS Aeronaut. J. **7**(1), 121 (2016)

55. Pohya, A.A., Wicke, K., Hartmann, J.: Comparison of direct operating cost and life cycle cost-benefit methods in aircraft technology assessment, in Proc 2018 AIAA Aerospace Sciences Meeting. AIAA Scitech Forum, Kissimmee (2018)

56. Ploetner, K.O., Schmidt, M., Baranowski, D., Isikveren, A.T., Hornung, M.: Operating cost estimation for electric-powered transport aircraft, in Proc 2013 Aviation Technology, Integration, and Operations Conference. AIAA Aviation Forum, Los Angeles (2013)

57. IATA: Jet fuel price monitor (2020). https://www.iata.org/en/publications/economics/fuel-monitor/ [Accessed: 03/08/2020]

58. Allgemeiner Deutscher Automobil-Club e.V.: Aktuelle Elektroautos im Test: So hoch ist der Stromverbrauch (2020). https://www.adac.de/rund-ums-fahrzeug/tests/elektromobilitaet/stromverbrauch-elektroautos-adac-test/?redirectId=quer.Elektroautos%20Ecotest [Accessed: 14/08/2020]

59. Federal Aviation Administration: FAA Aerospace Forecast – Fiscal Years 2020-2040 (2020). https://www.faa.gov/data_research/aviation/aerospace_forecasts [Accessed: 14/08/2020]

60. U.S. Energy Information Administration: Annual energy outlook 2020 (2020). https://www.eia.gov/outlooks/aeo/data/browser/#/?id=1-AEO2020&region=0-0&cases=ref2020&start=2019&end=2040&f=A&linechart=~ref2020-d112119a.41-1-AEO2020~&map=&ctype=linechart&sourcekey=0 [Accessed: 14/08/2020]

61. Haller, M., Loreck, C., Graichen, V.: Projected EEG costs up to 2035 – impacts of expanding renewable energy according to the long-term targets of the Energiewende. Tech. Rep. 079/14-S-2015/EN, Öko-Institut e.V., Freiburg (2016)

62. Nykvist, B., Sprei, F., Nilsson, M.: Assessing the progress toward lower priced long range battery electric vehicles. Energ policy **124**, 144 (2019)

63. IATA: Labor rate and productivity calculations for commercial aircraft maintenance. Tech. rep., International Air Transport Association, Montreal (2013)

64. AEA: Short medium range aircraft: AEA requirements. Association of European Airlines, Brussels (1989)

65. Gudmundsson, S.: General aviation aircraft design – applied methods and procedures. Butterworth-Heinemann, Amsterdam (2014)

66. Finger, D.F., Goetten, F., Braun, C., Bil, C.: Cost estimation methods for hybrid-electric general aviation aircraft, in Proc 2019 Asia-Pacific International Symposium on Aerospace Technology. Gold Coast (2019)

67. European Commission: Electricity price for non-household consumers, second half 2019 (2020). https://ec.europa.eu/eurostat/statistics-explained/index.php?title=File:Electricity_prices_for_non-household_consumers,_second_half_2019_(EUR_per_kWh).png [Accessed: 03/08/2020]

68. Swedavia AB: Airport Charges & Conditions of services (2020). https://www.swedavia.com/globalassets/flygmarknad/airpo

rt_charges_and_conditions_of_services_2020.pdf [Accessed: 14/08/2020]

69. European Environment Agency: The EU Emissions Trading System in 2019: trends and projections (2019). https://www.eea.europa.eu/themes/climate/trends-and-projections-in-europe/trends-and-projections-in-europe-2019/the-eu-emissions-trading-system/#_ftn5 [Accessed: 14/08/2020]

70. European Commission: EU Emission Trading Scheme, Allowance Allocation to Aviation (2020). https://ec.europa.eu/clima/policies/ets/allowances/aviation_en [Accessed: 14/08/2020]

71. OECD: Economic Outlook No 103, long-term baseline projection (2018). https://stats.oecd.org/Index.aspx?DataSetCode=EO103_LTB# [Accessed: 03/08/2020]

72. Kendall, M.: EU proposal for a directive on the establishment of a community framework for noise classification of on civil subsonic aircraft for the purposes of calculating noise charges, European Union (2003)

73. European Civil Aviation Conference: Recommendation ECAC/27-4 (second edition) – NOx emission classification scheme (2012)

74. Niklaß, M.: A systematic approach to internalising the climate impact of aviation [Ein systematischer Ansatz zur Internalisierung der Klimawirkung der Luftfahrt]. Ph.D. thesis, Technical University of Hamburg, Hamburg (2019)

75. Pornet, C., Isikveren, A.T.: Conceptual design of hybrid-electric transport aircraft. Prog. Aerosp. Sci. **79**, 114 (2015)

76. Pornet, C.: in New Applications of Electric Drives, ed. by Chomat, M. (IntechOpen, 2015), chap. 5, pp. 115–141

77. Iwanizki, M., Randt, N.P., Sartorius, S.: Preliminary design of a heavy short- and medium-haul turboprop-powered transport aircraft, in Proc 52nd Aerospace Sciences Meeting. AIAA Scitech Forum, National Harbor, Mariland (2014)

78. Hornung, M., Isikveren, A.T., Cole, M., Sizmann, A.: Ce-Liner - case study for emobility in air transportation, in Proc 2013 Aviation Technology, Integration, and Operations Conference. AIAA, Los Angeles (2013)

79. Schäfer, K.: Conceptual aircraft design for sustainability. Ph.D. thesis, RWTH Aachen University, Aachen (2018)

80. Howe, S., Kolios, A., Brennan, F.: Environmental life cycle assessment of commercial passenger jet airliners. Transport Res D-Tr E **19**, 34 (2013)

81. Timmis, A.J., Hodzic, A., Koh, L., Bonner, M., Soutis, C., Schäfer, A.W., Dray, L.: Environmental impact assessment of aviation emission reduction through the implementation of composite materials. Int. J. Life Cycle Ass. **20**, 233 (2015)

82. Fernandes Lopes, J.V.D.O.: Life cycle assessment of the Airbus A330-200 aircraft. Master's thesis, Universidade Técnica de Lisboa, Lisbon (2010)